ARTIGO ORIGINAL
DOI: 10.5433/1679-0375.2017v38n2p59

Efeito da Espessura na Banda de Absorção Óptica de Filmes Finos de V_2O_5 Depositados por Evaporação Térmica

Thickness Effect on the Optical Band Gap of V_2O_5 Thin Films Deposited by Thermal Evaporation

Luís Henrique Cardozo Amorin[1]; Larissa da Silva Martins[2];
Fábio Lopes[3]; Alexandre Urbano[4];

Resumo

Filmes finos de V_2O_5 têm sido usados como eletrodo passivo para ser aplicado em dispositivos eletrocrômicos que requer determinadas propriedades óptica, cristalográfica e de energia eletroquímica. Essas propriedades são influenciadas pela espessura do filme. Neste trabalho foram determinadas a dependência da espessura, a absorção óptica espectral e o tamanho de partícula dos filmes finos de V_2O_5 depositados por evaporação térmica com três espessuras nanométricas. A partir dos resultados, ficou claro que esses tamanhos de partículas, aparentemente, não são influenciados pela espessura do filme em sua formação. Assim, verificou-se que a microestrutura, principalmente a espessura, influencia fortemente as propriedades ópticas, especialmente a energia de absorção, dessas amostras. A energia de gap óptico diminui à medida que a espessura do filme aumenta. Isso realmente prova que a espessura do filme pode ser usada como forma de modular a absorção óptica de materiais em dispositivos ópticos e optoeletrônicos.
Palavras-chave: Band gap. Óxido de vanádio. Evaporação térmica. Filmes finos.

Abstract

Thin V_2O_5 films have been used as a passive electrode to be applied in some electrochromic devices that requires particular optical, crystallographic and electrochemical energy properties. These properties are greatly influenced by the film thickness. In this work were determined the thickness dependence on, spectral optical absorption and particle size of the V_2O_5 thin films deposited by thermal evaporation in three nanoscale thickness. It is clear from the results that these particles size apparently are not influenced by the thickness of the film in its formation. Thus, it was verified that the microstructure, mainly the thickness, strongly influences the optical properties, especially the absorption energy, of these samples. The optical gap energy decrease as the film thickness increased. This actually proves that film thickness can be used as a way to modulate the materials optical absorption in optical and optoelectronic devices.
Keywords: Band gap. Vanadium oxide. Thermal evaporation. Thin films.

[1]PhD Studant, Department of Physics, Universidade Estadual de Londrina; luis.amorin@gmail.com.
[2]PhD Studant, Department of Physics, Universidade Estadual de Londrina; la_smartins@hotmail.com.
[3]Physicist, Department of Physics, Universidade Estadual de Londrina; fabiolopes@uel.br
[4]Professor, Department of Physics, Universidade Estadual de Londrina; aurbano@uel.br

Introduction

Vanadium pentoxide (V_2O_5) is a transition metal oxide that is mainly considered as a typical intercalation compound, due to its orthorhombic structure (BEKE, 2011). During the past decades, V_2O_5 thin films have attracted significant attention in solar cell windows and electrochromic displays (TALLEDO; GRANQVIST, 1995; LIU et al., 2003; Panagopoulou et al., 2017), secondary lithium ion batteries electrode (Bhatt; O'Dwyer, 2015; Liang et al., 2016), electrochemical supercapacitors (Saravanakumar; Purushothaman; Muralidharan, 2012) and recently, V_2O_5 has been used for the NiO_2 gas detection (MANE et al., 2017; Huotari; LAPPALAINEN, 2017). The deposition technique used, the thickness and the crystalline structure of these films have a strong influence on the optical, electrical and mechanical characteristics of these materials (Mrowiecka et al., 2007).

Some studies have been described the films characterization with a thickness greater than 160 nm, but do not refer to the material crystalline structure study and its dependence on the thickness (KRISHNA; BHATTACHARYA, 1997).Others studies have been described the crystalline structure and the thickness effects on the optical properties only in films with thickness above 110 nm (RAMANA; SMITH; HUSSAIN, 2003; SINGH; KAUR, 2008; Zhang; Zuo; Lu, 2017) and another the influence of the sputtering power on the optical, electrical and nanomechanical properties for films (Porwal et al., 2015). Thus, no study was found relating the thickness and microstructure of films deposited by thermal evaporation with the optical absorption band. Especially, films with thickness less than 110 nm.

Nanoscale materials, such as thin films, the microstructure characterization is required, particularly particle size (D) and microstrain (ε). The particle size can be calculated using the Scherrer equation (Azaroff; BUERGER, 1958):

$$D = \frac{k\lambda}{\beta\cos(\theta)}, \tag{1}$$

where k is the coefficient of form for the reciprocal lattice and crystal form coefficient for the direct space,λ is the wavelength of the incident radiation, β is the width at half height of the peak (FWHM) and θ is the angle of Bragg (Cullity, 1978).

The microstrain (ε) measures how much the crystal moves away from the condition of perfection, being able to be written as (BURTON et al., 2009):

$$2\varepsilon = \left|\frac{\Delta d}{d}\right|. \tag{2}$$

Thus, the line width caused by the microstrain is given by:

$$\beta_\varepsilon = 4\varepsilon\tan(\theta), \tag{3}$$

where β_ε is the microstrain contribution for the width at half height of the peak. A simple method for separating the particle size and microstrain contributions in the diffraction peak line width is the Williamson-Hall graph (Williamson; Hall, 1953). This graph assumes the contributions of the diffraction peaks relative to particle size and microstrain. Combining equations 1 and 3, the Williamson-Hall equation can be written as:

$$\frac{\beta}{\lambda}\cos(\theta) = \frac{k}{D} + \frac{4\varepsilon}{\lambda}\sin(\theta), \tag{4}$$

where $\beta_{2\theta} = \beta_D + \beta_\varepsilon$ that is, a sum of the contributions of particle size and microstrain, respectively. For the Scherrer equation a Gaussian function to adjust the shape of the diffraction peak was used and was considered the form factor $k = 0.9$ (PATTERSON, 1939; Weibel et al., 2005; Gonçalves et al., 2012). For a Gaussian function the value of the width at half height of the peak $(\beta_{2\theta})$ of the Scherrer equation was obtained from the square root of FWHM of the sample measure $(\beta_{\exp})$ less an the FWHM contribution of the diffraction X-ray equipment $(\beta_{standard})$, as in equation 5. The $\beta_{standard}$ value was 0.07^o (0.0012 rad). The $\beta_{standard}$ value was obtained with the diffractogram of a polycrystalline silicon sample using the same measurements configurations.

$$\beta_{2\theta} = \sqrt{\beta_{\exp}^2 - \beta_{standard}^2} \tag{5}$$

Thus, through the Williamson-Hall graph, particle sizes and microstrains were calculated for thin films of V_2O_5 deposited with different thickness by the thermal evaporation technique, and subsequently, heat treated. This difference in film thickness was compared with the variation in the optical absorption band of the material.

Experimental

The thin films of vanadium oxide were deposited by high vacuum evaporation in a HHV model AUTO 306 using a tungsten boat as a source of evaporation. The oxide to be evaporated was made into pellets by uniaxial pressing of 100mg, 70mg and 35mg of V_2O_5 powder (SIGMA-ALDRICH, $\geq$ 99.6 %) using a Potente Brasil hydraulic press with 5 ton of load. Glass plates coated with indium tin oxide (ITO) film were used as substrates. The

substrates were cleaned in ultrasonic acetone followed by isopropanol baths solutions and heated at 100 °C within the high vacuum deposition chamber to degasify their surface. At the time of deposition, the substrates were kept at room temperature. The base pressure measured with a Penning-type sensor was $7.89x10^{-6}$ mbar and the working pressure is $1.15x10^{-5}$ mbar. Thin films of V_2O_5 with different thickness were obtained from different depositions, in which all material added in the boat was evaporated. The deposited thin films were heat-treated ex-situ at 400 °C, with control and 3 °C/min for both heating and cooling, for 2 hours under atmospheric oxygen (99.99999 %).

The thickness of the deposited films was analyzed by a portable X-ray fluorescence (PXRF) system using the attenuation of the intensity of the $K\alpha$ radiation of the calcium present in the glass substrate, Figure 1. The measurements were done using a MAGNUM MUHV Mini X-ray tube manufactured by Moxtec (Moxtec Inc.) with both silver targets (Ag). This tube can be operated in up to 40 kV and 100 μA with a maximum power of 4 W, for a better system performance Ag filter was used. A XR-100CR Si-PIN detector with a preamplifier, a thermoelectric cooling system, a conjugated high- tension source module, and an amplifier was also employed, connected to a multichannel analyzer model MCA8000A (Amptek Inc.).

Figure 1 – Schematic of the $CaK\alpha$ attenuation for the film thickness measurement.

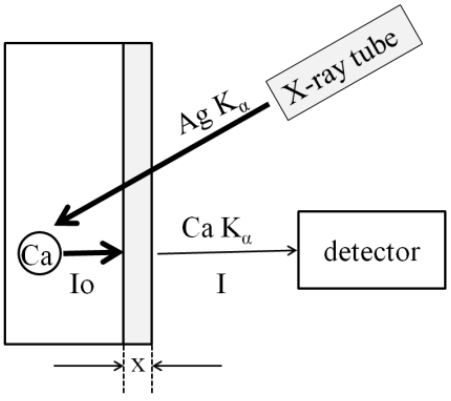

Source: The Author.

The X-ray diffraction measurements were performed on a Bruker D8 diffractometer with CuKα radiation ($\lambda =$ 1.5405 Å) focusing on a line energized by a voltage of 40 kV and current of 40 mA Bragg-Brentano geometry. The angle range (2θ) was from 18 to 28°, with a step width of 0.05° and data collection time of 5 s per step.

The crystallite size and the microstrain were obtained by the Williamson-Hall method expressed by equation 4. The band gap energy of the V_2O_5 thin films was obtained by the Tauc ratio (WOOD; TAUC, 1972) by means of optical measurements using a spectrophotometer Perkin-Elmer lambda 1050 WB, with a wavelength in the range of 300 to 1200 nm that is showed in Figure 2.

Figure 2 – Optical transmittance measurements schematic for obtain the band gap energy.

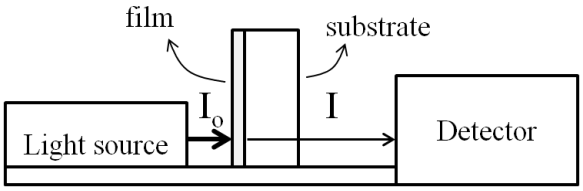

Source: The Author.

Results and Discussions

The structural and morphological measurements of the samples are extremely important since from the analysis of these parameters it is possible to correlate how the formation of the film on the substrate and its consequences on the optical responses of the film occurs. The three samples with different masses were analyzed at three different points. To consider a vanadium thin film simple case deposited on a glass flat surface (substrate), the film thickness could be determined by the measurement of constituent substrate element attenuation intensity. The results found for the thickness and surface density of the V_2O_5 films, together with their respective deviations for the three samples, are shown in table 1.

Table 1 – The V_2O_5 film thickness calculated by the attenuation of the calcium line Kα.

Mass (mg)	Net peak Area of Ca-Ka (arbit. unit)	Thickness (nm)	Superficial Density (g/cm^2)
35 ± 3	10008	50 ± 7	16.1 ± 3
70 ± 3	9081	110 ± 3	36.9 ± 3
100 ± 3	8501	160 ± 5	53.7 ± 4

Source: The Author.

The intensity of the Ca-Kα line was determined for the spectrum obtained by PXRF. The Ca-Kα spectral line was chosen because it was the most intense spectral line emitted by the substrate. The corresponding film thickness was calculated using the equation obtained from a calibration curve (LOPES et al., 2016). Thus, assuming

that a thin film with a nanometric vanadium thickness is deposited on a substrate of another element (Ca), the measured intensity for the X-rays in which characteristic of the Ca-Kα was exponentially attenuated, according to the radiation attenuation law.

The diffractograms of the samples are shown in Figure 3. The samples 160 nm, 110 nm and 50 nm are the thin films of V_2O_5 deposited with these thicknesses, respectively. In the thicker films, the peak (010) characteristic of the V_2O_5 orthorhombic phase (ICSD – 01-075-0457) is verified.

Figure 3 – X-ray diffraction of V_2O_5 thin films with different thickness.

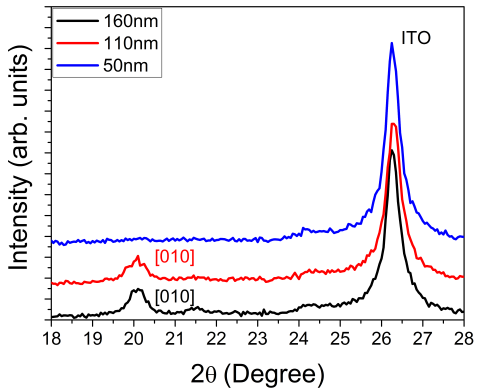

Source: The Author.

A variation in the intensity of the diffracted peak is observed as the thickness of the films is changed. This can be better visualized by analyzing only the peak (010) of the diffractogram. It can be clearly observed the decrease of the peak with the thickness variation, Figure 4. A second peak (110) is also observed with the same characteristics of the peak (010). Having the diffractogram peaks defined according to Figure 4, one can calculate the width at half height of the peaks. Although slightly perceptible, the peak has a half-height (FWHM) which allows to calculate the grain size using the Scherer equation for the (110) peak and also permits the use of this point to calculate the grain size by Williamson-Hall technique. From the FWHM it is possible to characterize the microstructure of nanoscale materials.

The practical application of the Williamson-Hall graph, Figure 5, consists of constructing a $\beta\cos(\theta/\lambda)$ versus $\sin(\theta)$ graph. This graph was constructed for the thin films with the different thickness, 160, 110 and 50 nm, from the FWHM of the peaks identified in the diffractograms, Figure 4.

Analyzing the graph, Figure 5, different slopes for the different thickness are observed. The slope of the lines

Figure 4 – X-ray diffraction patterns showing the FWHM value for the diffracted peaks.

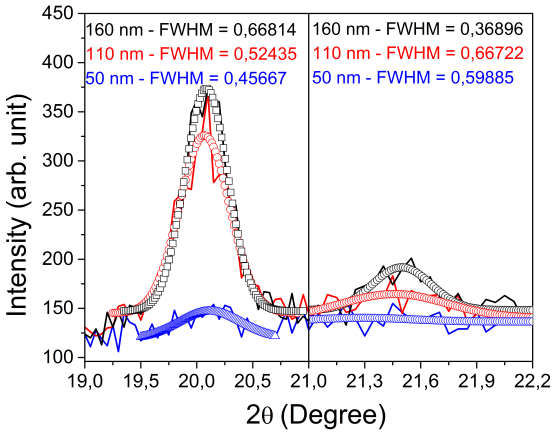

Source: The Author.

Figure 5 – Williamson-Hall plot obtained through the values found for samples FWHM.

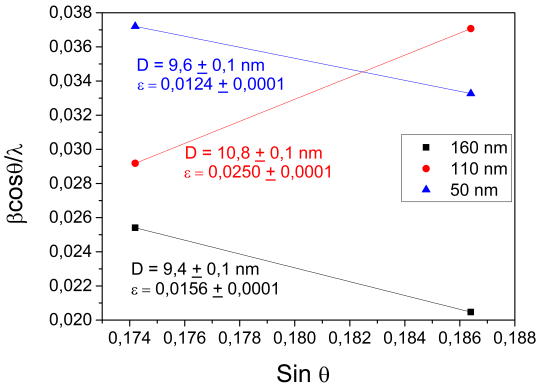

Source: The Author.

is related to the microstrain in the crystalline structure of the samples. For the ascending lines, an expansion of the structure is attributed in the direction of the diffraction peak. The downlines indicate a compression of the structure in the direction of the diffraction peak. No deformations occur in the structure, that is, indicating a perfect crystal, the line remains horizontal to the abscissa axis of the graph (Gonçalves et al., 2012).

This graphical method provides the particle size and microstrain value of the thin film forming crystals. For the film with a thickness of 160 nm, the ε is 156 times larger than the crystalline silicon, Si (0.01%), which is a free sample of microstrains (Gonçalves et al., 2012). The descending character of the curve shows a compression of the film structure. For the film with a thickness of 110 nm, the strain is 250 times larger than the standard was obtained and the upward curve is observed, characterizing an expansion of the film structures. Finally, for the less thick film, 50 nm, the microstrain is 124 times larger than

the Si standard and this sample also shows a downward curve profile, showing a compression of the film structure. Due to the formation of the morphological structure of the film at the time of deposition, according to the Thornton Diagram (Thornton, 1977) an intrinsic mechanical tension of the structure occurs. Thus, our results seem to demonstrate a dependence of this mechanical tension with the thickness of the film.

The particle sizes calculated by the Williamson-Hall method for 160, 110 and 50 nm thick films are 9.6, 10.8 and 9.4 nm, respectively. These values found from the Williamson-Hall chart are very close to those calculated through the Scherrer equation. According to Gonçalves and collaborators (Gonçalves et al., 2012), the values of D calculated by the Scherrer equation must be corrected through the microstrain in the value of β, using the equation (3). The obtained particle sizes show that the films are practically homogeneous, and also that there is no relation of the particle size to the film thickness. The values for D calculated by the Scherrer equation are shown in table 2.

For the samples with 160 and 50 nm, a good relation between the graphical technique and theoretical calculation, equation 1 with the corrected β value, is observed. The discrepancy between the values calculated through the Scherrer equation and the values obtained through the Williamson-Hall plot, for D in the 110 nm thick film, can be understood due to the lack of diffraction peaks of the samples, consequently, the lack of points in the construction of the Williamson-Hall chart. This characterization of the microstructure of the film is fundamental since the particle size and the microstrain can alter the material physical properties.

One of the physical properties influenced by the microstructure of thin films is the variation in the optical absorption band of the material. To estimate the absorption band, one can start from the spectral absorption coefficient of the film, assuming that the spectral reflectance is close to zero, will be given by (Chopra; Mansingh; Chadha, 1990):

$$\alpha = -\frac{1}{x}\ln(T), \tag{6}$$

where T is the transmittance of radiation by the material, α is the absorption coefficient and x is the sample thickness. The coefficient of optical absorption as a function of the wavelength of the incident radiation is shown in Figure 6.

As can be seen in Figure 6, the increase in the absorption coefficient can be clearly observed with the decrease in film thickness. The decrease in the band gap and changes in the spectral characteristics are attributed

Figure 6 – Spectrum of the optical absorption coefficient and spectral transmittance as a wavelength function.

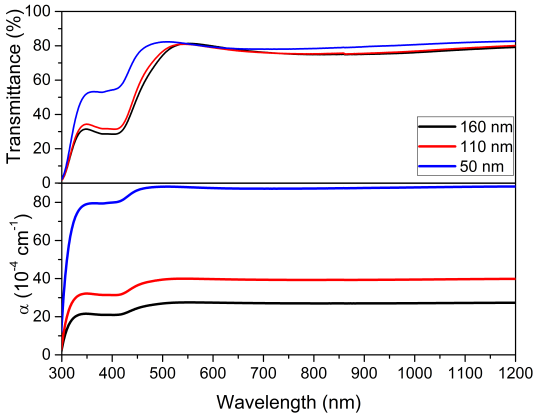

Source: The Author.

to the increase in the grain size, random grain distribution, and structural modification of the material in the films (RAMANA; SMITH; HUSSAIN, 2003, RAMANA et al., 2005). The variation of the absorption coefficient with the energy of the incident photon is given by the relation of Tauc (WOOD; TAUC, 1972):

$$\alpha E = (E - E_g)^n, \tag{7}$$

where E is the energy of the incident photon, E_g is the energy of the optical absorption band and n is a constant referring to the type of electronic transition in the material. From equation 7 the optical gap energy (E_g) can be estimated when $\alpha E = 0$. For this was constructed the graph of $(\alpha E)^{1/2}$ versus the incident photon energy, to calculate the gap energy was extrapolated a line to the point that cuts the abscissa axis $(\alpha E = 0)$, according to Figure 7.

Figure 7 – Curve of $(\alpha E)^{1/2}$ versus Energy and the extrapolation of a straight line to the point that cuts the abscissa axis $(\alpha E)^{1/2} = 0$.

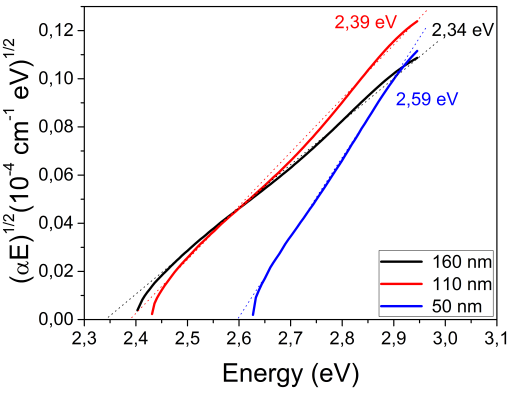

Source: The Author.

The values calculated by the ratio of Tauc to Eg were found to be 2.59, 2.39 and 2.34 eV for samples with

Table 2 – Particle size of the samples calculated by the Scherrer equation and by Williamson-Hall plot.

Film Thickness (nm)	Scherrer Equation D(nm)		Williamson-Hall Plot	
	hkl (010)	hkl (110)	D(nm)	$\varepsilon(\%)$
160	8.2 ± 0.4	9.2 ± 0.4	9.4 ± 0.1	0.0156 %
110	6.3 ± 0.4	5.7 ± 0.4	10.8 ± 0.1	0.0250 %
50	10.7 ± 0.4	9.4 ± 0.4	9.6 ± 0.1	0.0124 %

Source: The Author.

thickness of 50, 110 and 160 nm, respectively. These values are very close to those reported in the literature (Ramana; SMITH; HUSSAIN, 2003; KRISHNA; BHATTACHARYA, 1997).

Conclusions

In this work, V_2O_5 thin films with different thickness (50, 110 and 160 nm), prepared by thermal evaporation, were submitted to an analysis of its microstructure and its optical properties. Microstructural analysis using the X-ray diffraction technique showed that the films are formed by particles with an average size of 10 nm, these particles apparently are not influenced by the thickness of the film in its formation. Thus, it was verified that the microstructure, mainly the thickness, strongly influences the optical properties, especially the absorption energy, of these samples. The optical gap energy varied from 2.59 to 2.34 eV as the film thickness increased. This actually proves that film thickness can be used as a way to modulate the materials optical absorption in optical and optoelectronic devices. Thus, altering its optical properties, such as the optical absorption coefficient, the index of refraction and the extinction coefficient, furthermore its transmittance and reflectance.

Acknowledgements

To the Semiconductor Film Laboratory of the Universidade Estadual Paulista, UNESP for the optical absorption measurements and to the Multi-user Laboratory of the Gleb Wataghin Physics Institute of the Universidade Estadual de Campinas, UNICAMP, for X-ray diffraction measurements.

Reference

Azaroff, L. V.; BUERGER, M. J. *The powder method in X-ray crystallography*. New York: McGraw-Hill Book Co. Inc., 1958. 342 pp.

BEKE, S. *A review of the growth of V_2O_5 films from 1885 to 2010*. Thin Solid Films, v. 159. p. 1761-1771, 2011.

Bhatt, M. D.; O'Dwyer, C. *Recent progress in theoretical and computational investigations of Li-ion battery materials and electrolytes*. Physical Chemistry Chemical Physics, v. 17, n. 7, p. 4799-4844, 2015.

Burton, A. W.; Ong, K.; Rea, T.; Chan, I. Y. *On the estimation of average crystallite size of zeolites from the Scherrer equation: a critical evaluation of its application to zeolites with one-dimensional pore systems*. Microporous Mesoporous Mater, v. 117, p. 75-90, 2009.

Chopra, N.; Mansingh, A.; Chadha, G. K. *Electrical, optical and structural properties of amorphous V_2O_5-TeO_2 blown films*. J. Non. Cryst. Solids, v. 126, p. 194-201, 1990.

Cullity, B. D. *Elements of X-ray diffraction*. 2^{nd} edition. Philippines, Addison-Wesley Publishing Company, 1978.

Gonçalves, N. S.; Carvalho, J. A.; Lima, Z. M.; Sasaki, J. M. *Size-strain study of NiO nanoparticles by X-ray powder diffraction line broadening*. Materials Letters, v. 72, p. 36-38, 2012.

Huotari, J.; Lappalainen, J. *Nanostructured vanadium pentoxide gas sensors for SCR process control*. Journal of Materials Science, v. 52, n. 4, p. 2241-2253, 2017.

KRISHNA, M. G.; BHATTACHARYA, A. K. *Effect of thickness on the optical absorption edge of sputtered vanadium oxide films*. Materials Science and Engineering B, v. 49, p. 166-171, 1997.

Liang, X., Gao, G., Liu, Y., Ge, Z., Leng, P., Wu, G.; *Carbon nanotubes/vanadium oxide composites as cathode materials for lithium-ion batteries*. Journal of Sol-Gel Science and Technology, v.82 n 1, p. 224-232, 2016.

LIU, P.; LEE, S. H.; TRACY, C. E.; TURNER, J. A.; PITTS, J. R.; DEB, S. K. *Electrochromic and chemochromic performance of mesoporous thin-film vanadium oxide*. Solid State Ionic, v. 165, p. 223- 228, 2003.

Lopes, F.; Amorin, L. H. C.; MARTINS, L. S.; Urbano, A.; Appoloni, C. R.; Cesareo, R., "*Thickness Measurement of V_2O_5 Nanometric Thin Films Using a Portable XRF*," Journal of Spectroscopy, vol. 2016, Article ID 9509043, 7 pages, 2016.

Mane, A. A.; Suryawanshi, M. P.; Kim, J. H.; Moholkar, A. V. *Fast response of sprayed vanadium pentoxide (V_2O_5) nanorods towards nitrogen dioxide (NO_2) gas detection*. Applied Surface Science, v. 403, p. 540-550, 2017.

Mrowiecka, J. S.; Maurice, V.; Zanna, S.; Klein, L.; Vickridge, E. B. I.; Marcus, P. J. *Ageing of V_2O_5 thin films induced by Li intercalation multi-cycling*. Power Sources, v. 170, p. 160, 2007.

Panagopoulou, M., Vernardou, D., Koudoumas, E., Tsoukalas, D., Raptis, Y. S.; *Oxygen and temperature effects on the electrochemical and electrochromic properties of rf-sputtered V_2O_5 thin films*. Electrochimica Acta, v. 232, p. 54-63, 2017.

PATTERSON, A. L. *The Scherrer formula for X-Ray particle size determination*. Physical Review, v. 56, n. 10, p. 978-982, 1939.

Porwal, D.; Esther, A. C. M.; Reddy, I. N.; Sridhara, N.; Yadav, N. P.; Rangappa, D.; Bera, P.; Anandan, C.; Sharma, A. K.; Dey, A. *Study of the structural, thermal, optical, electrical and nanomechanical properties of sputtered vanadium oxide smart thin films*. RSC Advances, v. 5, n. 45, p. 35737-35745, 2015.

RAMANA, C. V.; SMITH, R. J.; HUSSAIN, O. M. *Grain size effects on the optical characteristics of pulsed-laser deposited vanadium oxide thin films*. Physica Status Solidi (a), v. 199, n. 1, p. R4-R6, 2003.

RAMANA, C. V. ; SMITH, R. J.; HUSSAIN, O. M., CHUSUEI, C.C., JULIEN, C.M., *Correlation between growth conditions , microstructure , and optical properties in pulsed-laser-deposited V_2O_5 thin films*. Society, v. 405, n. 5, p. 1213-1219, 2005.

Saravanakumar, B.; Purushothaman, K. K.; Muralidharan, G. *Interconnected V_2O_5 nanoporous network for high-performance supercapacitors. ACS Applied Materials & Interfaces*, v. 4, n. 9, p. 4484-4490, 2012.

Singh, P.; Kaur, D. *Influence of film thickness on texture and electrical and optical properties of room temperature deposited nanocrystalline V_2O_5 thin films*. J. Appl. Phys. v. 103, p. 1-8, 2008.

TALLEDO, A.; GRANQVIST, C. G.; *Electrochromic vanadium-pentoxide-based films: Structural, electrochemical, and optical properties*. J. Appl. Phys, v. 77, n. 9, p. 4655-4666, 1995.

Thornton, J. A. High rate thick film growth. *Annual Review of Materials Science*, v. 7, n. 1, p. 239-260, 1977.

Weibel, A.; Bouchet, R.; Boulc'h, F.; Knauth, P. *The big problem of small particles: a comparison of methods for determination of particle size in nanocrystalline anatase powders*. Chem. Mate, v. 17, p. 2378-2385, 2005.

Williamson, G. K.; Hall, W. H. *X-ray line broadening from filed aluminum and wolfram*. Acta Metall, v. 1, p. 22-31, 1953.

WOOD, D. L.; TAUC, J. *Weak absorption tails in amorphous semiconductors*. Physical Review B, v. 5, n. 8, p.3144-3151, 1972.

Zhang, S. B.; Zuo, D. W.; Lu, W. Z. *Influence of film thickness on structural and optical-switching properties of vanadium pentoxide films*. Surface Engineering, v. 33, n. 4, p. 292-298, 2017.

Recebido em 30 Março, 2017– Received on March 30, 2017
Aceito em 14 Julho, 2017– Accepted on July 14, 2017